nature portfolio

https://doi.org/10.1038/s41564-022-01227-4

Supplementary information

Computational identification of a systemic antibiotic for Gram-negative bacteria

In the format provided by the authors and unedited

Supplementary Information

Supplementary Notes

Cryo-EM MicroED

The compound crystallized in space group C2 with one molecule in the asymmetric unit, and the structure was solved by *ab initio* direct methods in SHELXT, followed by refinement in SHELXL[62]. The crystal packing is dominated by antiparallel β-sheet arrangements between adjacent molecules (**Extended Data Figure 3C**), with the polypeptide strands related by a crystallographic 2_1 screw axis (parallel to the b axis of the crystal), and the directions of the strands oriented normal to this direction.

A critical question in the diffraction analysis was establishing the orientation of the His^6 sidechain, as the crosslink with Tyr^8 Cβ could involve either the side chain Nε2 or Cε2 atom. In view of the similarities of the electron scattering factors for these two elements, it was not possible to unambiguously distinguish these two possibilities through the crystallographic analysis. The assignment of the His^6 sidechain orientation supporting the role of Nε2 in the crosslink was based on comparison of the sidechain bond angles to those observed in small molecule structures in the Cambridge Structure Database[80]. In this study, the extracyclic Cβ-Cγ-Cδ and Cβ-Cγ-Nδ bond angles in the different protonated forms of the histidine side chain were found to be 130˚ and 123˚, respectively; in the refined dynobactin A structure, these are 127.4˚ and 122.5˚, respectively. Flipping the ring orientation (corresponding to participation of the Cε atom in the crosslink) would interchange the Nδ and Cδ atoms and hence would be inconsistent with the small molecule bond angle observations.

The planes of the two macrocyclic rings are approximately perpendicular to one another. The polypeptide torsion angles of dynobactin are in the β-strand region of the Ramachandran plot, with the exceptions of S^3 and N^4 in the left- and right-handed α-helix regions, respectively. The Cα-Cα spacings between alternate residues in the extended conformation of dynobactin (residues 5-10) average ~6.5 Å, which is close to that observed in the darobactin structure (6.5 Å for residues 1-7); the most significant difference is the compressed Cα-Cα spacing between residues H^6 and Y^8 of dynobactin (5.95 Å) reflecting the smaller crosslink involving the H^6 sidechain relative to the longer crosslinks involving the W^1 and W^3 sidechains in darobactin. In both dynobactin A and darobactin A, these crosslinks function to stabilize a pre-ordered β-strand conformation that can bind with high affinity to an exposed β-strand of the target protein. The final model contains the full dynobactin A decapeptide and 8 water molecules. As the net charge on dynobactin A is plausibly +1 (with a protonated N-terminal nitrogen and Arg^9 sidechain, and a negatively charged C-terminal carboxylate), electroneutrality requires a negatively charged counterion that is likely distributed among the water molecules or disordered.

Secondary Structural Confirmations, Marfey's Analysis

We also confirmed the structure of dynobactin A using two well-established approaches for natural product small molecules. First, dynobactin A was acid-hydrolyzed to break all peptide bonds and to liberate individual amino acids. Following this, Marfey's reagent was used to derivatize, separate, and identify these residues[81]. In this case, other N-C connections were also broken by the hydrolysis, liberating tyrosine from histidine, making a C-C closure in the second cyclophane ring extremely unlikely. This showed that both the amino acids and their chirality was consistent with the proposed microED structure (**Extended Data Figure 4**).

Secondary Structural Confirmations, NMR

In addition, nuclear magnetic resonance studies (NMR) provided a structural assignment (**Supplementary Table 4, Extended Data Figure 4**) by the detailed 1D (**Extended Data Figure 4A-B**) and 2D NMR analysis including COSY, ROESY, TOCSY, ^1H-^{13}C HSQC, and ^1H-^{13}C HMBC in both DMSO-d_6 and D_2O solvents (**Extended Data Figure 4C**). In the DMSO-d_6

sample, 15 spin systems were identified from COSY and TOCSY spectra, including 10 from the amino acid backbone, and 2 from the tryptophan side chain, two overlapping spin systems from the tyrosine side chain and one from the phenylalanine side chain. The α- and β-carbon and proton chemical shifts in each amino acid residue were identified by phase-sensitive ^{1}H-^{13}C HSQC experiments. Among the 10 amino acid backbone spin systems, eight showed α-protons connecting to a methylene, two showed α-protons connected to another methine. The D_2O sample provided additional ^{1}H-^{13}C HMBC correlations and the key 2D correlations are summarized in (**Extended Data Figure 4D**). The three aromatic side chains of tryptophan, tyrosine and phenylalanine were readily established by COSY and HMBC correlations. H-5 from the tryptophan side chain showed ^{3}J HMBC correlations to C-3 connecting the tryptophan side chain to the backbone spin system. Both H-13 and H-14 had an HMBC correlation to two carbonyl carbons C-12 and C15, establishing an asparagine moiety. H-2, H-3 and H-13 shared the same HMBC correlations to the carbonyl carbon C-1, connecting the tryptophan moiety and the asparagine moiety. Two spin systems H-17 and H-18, H-35 and H-36 had similar carbon and proton chemical shifts, and they were assigned as two serine side chains based on their characteristic β-carbon chemical shifts. Both H-17 and H-18 shared an HMBC correlation to C-16, while H-35 had an HMBC correlation to C-28. A second asparagine was identified based on HMBC correlations from H-20 to two carbonyl carbons C-19 and C-22; H-21 also has ^{2}J correlations to C-22. Interestingly, the β-carbon in the spin system was a methine instead of a methylene group based on phase sensitive HSQC signals, which suggested a substitution at the C-21 position. The HMBC ^{3}J correlations between H-7 and H-9 to C-21, and the ^{2}J HMBC correlation from H-21 to C-8 suggested the connectivity between C-8 and C-21, connecting the β-carbon of the asparagine to the side chain of tryptophan. The valine spin system was characterized by two methane signals; H-26 and C-27 shared a COSY correlation to a methine proton, C-25. The α-proton showed an HMBC correlation to C-19, connecting the valine moiety to the substituted asparagine. Both H-24 and H-25 shared an HMBC correlation to the carbonyl carbon C-23. The histidine moiety was characterized by two aromatic methine groups at positions 33 and 32, where H-33 had an HMBC correlation to C-32. The tyrosine side chain was connected to its backbone, shown by HMBC correlations from H-39 to C-41 and C-40, as well as from H-38 to C-40. The α-proton of tyrosine had HMBC correlations to two carbonyl carbons C-34 and C-37. Interestingly, the β position of tyrosine showed a methine group, instead of a methylene group, as evidenced by the phase-sensitive HSQC, suggesting a substitution at the β position. The key HMBC correlation from H-39 to C-32 established the connectivity between C-39 and the histidine side chain. In particular, the characteristic ^{13}C NMR chemical shift of C-39 (δ 63.4) strongly suggested carbon-nitrogen linkage. In addition, ROESY correlations between H-32 and H-38, as well as between H-32 and H-41 further confirmed the macrocyclic connection between tyrosine β-carbon, C-39, and the histidine side chain. Due to the HSQC correlation of both C-33 and C-32, C-39 must connect to a histidine side chain nitrogen atom. The assignment between C-39 and the nitrogen between C-32 and C-33 was based on cryo-EM microED 3D structure, indicating connection to an atom in the ε position on the histidine side chain, here meaning Nε2. The spin system consisting of C-47, C-48, C-49, and C-50 was assigned as arginine based on the characteristic methylene proton and carbon chemical shifts at C-50. In the end, HMBC correlations between H-54 to H-55 and H-56 established the phenylalanine moiety, and an HMBC correlation was observed between H-54 to the terminal carbonyl carbon C-52. The two serine side chain regions had limited HMBC correlations and the assignment of the backbone spin systems could be switched. The last backbone spin system consisting of C-29 and C-30 has to be assigned to histidine to complete the full structure, although no HMBC correlations between the side chain and the backbone was observed.

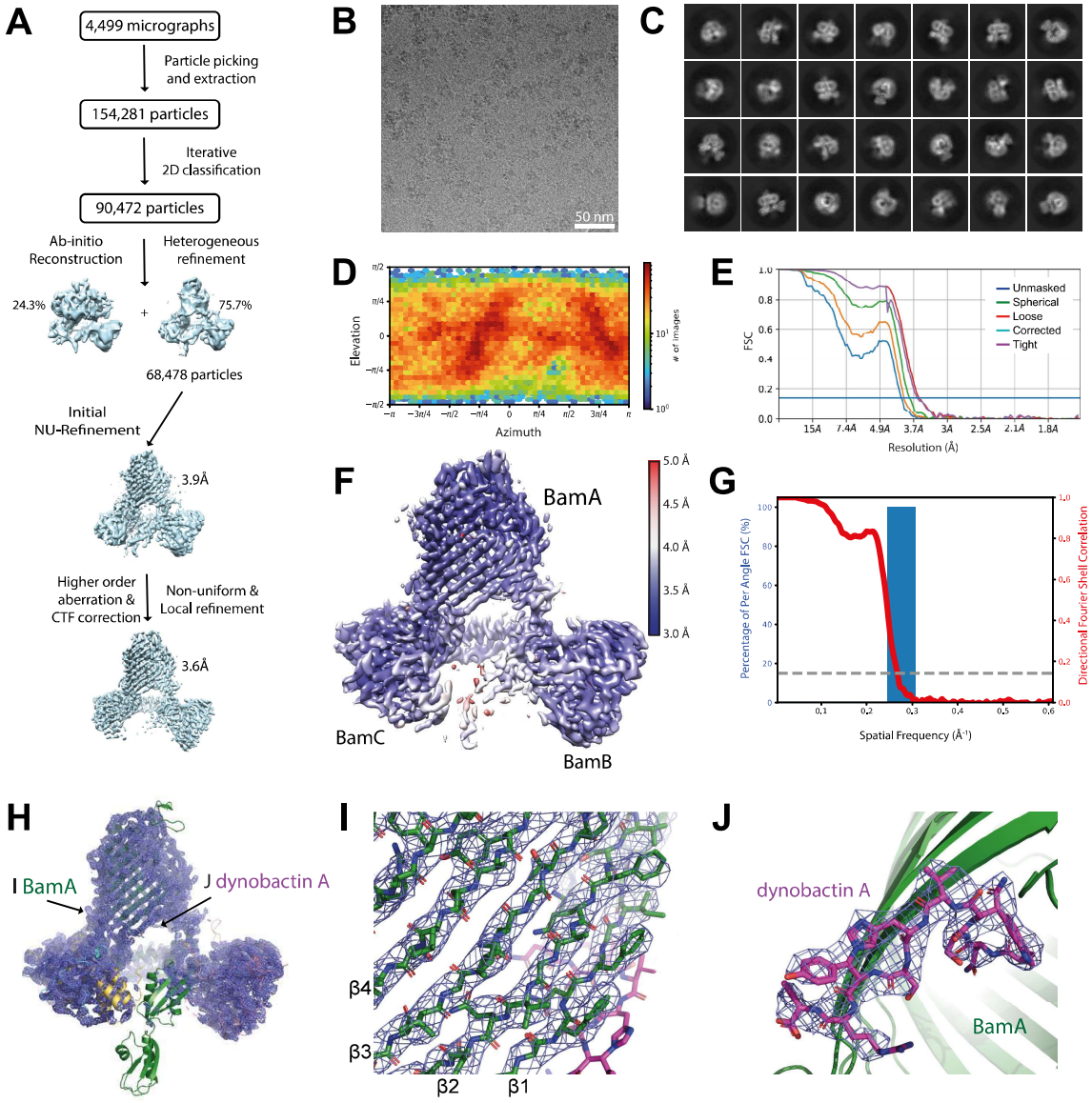

Supplementary Figure 1. Cryo-electron microscopy structure of the BAM–dynobactin A complex.

(A) Data processing flowchart to generate the cryo-EM map (see Materials & Methods). **(B)** Representative electron micrograph of BAM–dynobactin A **(C)** Examples of 2D classes from cryoSPARC. **(D)** Viewing direction distribution plot for the final 3D reconstruction. **(E)** Fourier shell correlation (FSC) curves for unmasked, spherical, loose, and tight masks, and corrected FSC curve for the final reconstruction, yielding a gold standard FSC resolution of 3.6 Å. **(F)** Local resolution variations of the EM reconstruction. POTRA domains 1 and 2 are at a local resolution below 5 Å and are visualized only at a lower contour level. **(G)** Directional FSC plot (red; mean ± SD) and histogram of per angle FSC (blue). The grey dotted line shows the FSC of 0.143, indicating a resolution of 3.75 Å. **(H)** Overview of the cryo-EM reconstruction of the BAM-dynobactin A complex. BAM is shown in ribbon representation and the coulomb potential map as slate blue mesh. Close-Up views showing the map around selected atoms in stick representation of **(I)** the BamA barrel and **(J)** dynobactin A.

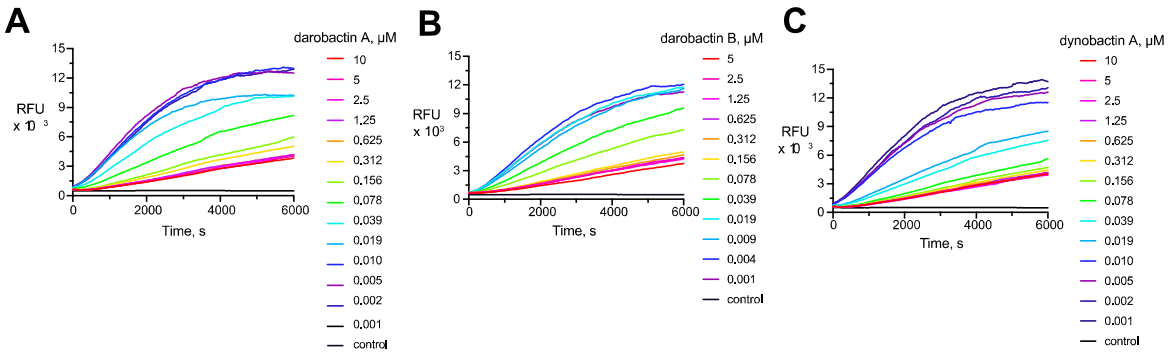

D

Compound	IC_{50} (nM)
Darobactin A	30 ± 6
Darobactin B	48 ± 8
Dynobactin A	16 ± 2

E

Compared Pair	F-ratio	p-value
Dynobactin A and Darobactin A	40.3	< 0.0001
Dynobactin A and Darobactin B	128	< 0.0001

Supplementary Figure 2. Inhibition of BAM-mediated OMP folding by darobactins and dynobactin A.

Fluorescence emission of BAM-mediated OmpT activity in presence of **(A)** darobactin A, **(B)** darobactin B, and **(C)** dynobactin A at variable compound concentration as indicated. From these data, the initial reaction rates were determined and plotted against the compound concentration to determine the IC_{50} values with a 95% confidence interval (**Extended Data Figure 6E**). **(D)** IC_{50} value and 95% confidence intervals, as determined by the BAM- mediated OmpT folding assay. **(E)** Significance test for shared IC_{50} for a pair of datasets implemented in GraphPad Prism with an extra sum-of-squares F-test. In both cases, the IC_{50} shows a significant difference between the datasets. Exact p-values for dynobactin A versus darobactin A and B were reported as 0.000000074 and 0.000000000000013, respectively.

Supplementary Tables

Strain	Sequence	Group	rSAM	Propeptide	SPASM Cys Motif
Clostridium perfringens	--	anSME	ABG83662.1	--	Cx5Cx9Gx4Cx40Cx2Cx5Cx3Cx17C
Photorhabdus australis	…ATIPS**WNSNVHSYRF**	Dynobactins	WP_065822265.1	WP_036772053.1	Cx5Cx10Gx4Cx39Cx2Cx5Cx3Cx18C
Pectobacterium polaris	…AAVPS**WNSNVHKYRF**	Dynobactins	WP_161546622.1	WP_161546621.1	Cx5Cx10Gx4Cx39Cx2Cx5Cx3Cx18C
Pandoraea terrae	…SSNFY**WIGNAHTYLF**…	Dynobactins	VVE19333.1	VVE19312.1	Cx5Cx10Gx4Cx39Cx2Cx5Cx3Cx18C
Pandoraea sp.	…VCSYH**WNGNVHTYHY**…	Dynobactins	VVE29655.1	VVE29677.1	Cx5Cx10Gx4Cx39Cx2Cx5Cx3Cx18C
Candidatus Berkelbacteria	…ICGDP**WSGNVYKYNF**	Dynobactins	MBI4032588.1	MBI4032587.1	Cx5Cx10Gx4Cx39Cx2Cx5Cx3Cx18C
Flavihumibacter petaseus	…MCGDP**WSGNIYRYNF**…	Dynobactins	WP_046371420.1	WP_046371421.1	Cx5Cx10Gx4Cx39Cx2Cx5Cx3Cx18C
Massilia sp.	…QSEPK**WKANIHSYSF**…	Dynobactins	HBZ07512.1	HBZ07511.1	Cx5Cx10Gx4Cx39Cx2Cx5Cx3Cx18C
Rhodothalassium salexigens	…ICEDP**WSGNIYRYSF**	Dynobactins	WP_132706374.1	WP_132706375.1	Cx5Cx10Gx4Cx39Cx2Cx5Cx3Cx18C
Vibrio parahaemolyticus	…FFGED**WTGNVYRYTS**	Dynobactins	WP_182021128.1	WP_182021129.1	Cx5Cx10Gx4Cx39Cx2Cx5Cx3Cx18C
Methylosarcina fibrata	…VCGDP**WSGNVYTYRF**…	Dynobactins	WP_157385903.1	WP_157385902.1	Cx5Cx10Gx4Cx39Cx2Cx5Cx3Cx18C
Photorhabdus temperata	…AASPG**WDGNIYKYSF**	Dynobactins	WP_023045852.1	WP_023045853.1	Cx10Gx4Cx39Cx2Cx5Cx3Cx18C
Xenorhabdus kozodoi	…AASPG**WDGNIYKYGF**	Dynobactins	WP_099142115.1	WP_167386578.1	Cx5Cx10Gx4Cx39Cx2Cx5Cx3Cx18C
Citrobacter sp.	…PNDAS**WDYNVHQWSY**…	Dynobactins	WP_075551248.1	WP_156174794.1	Cx5Cx10Gx4Cx39Cx2Cx5Cx3Cx18C
Sodalis sp.	…STVPS**WNSNVHKYRC**	Dynobactins	WP_213989350.1	WP_213989351.1	Cx5Cx10Gx4Cx39Cx2Cx5Cx3Cx18C
Akkermansiaceae bacterium	…DELLA**WEGNIYKYRF**…	Dynobactins	MBx3740458.1	MBx3740457.1	Cx5Cx10Gx4Cx39Cx2Cx5Cx3Cx18C
Saprospiraceae bacterium	…TSGGG**WKGNLHSWGF**…	Dynobactins	MBP7541614.1	MBP7541615.1	Cx5Cx10Gx4Cx39Cx2Cx5Cx3Cx18C
Photorhabdus khanii	…PKIPEITA**WNWSKSF**…	Darobactins	WP_036847505.1	WP_152962143.1	Cx5Cx10Gx4Cx42Mx2Cx5Cx3Cx17CC
Photorhabdus australis	…PKIPEITA**WNWSKSF**…	Darobactins	WP_036772804.1	WP_157835564.1	Cx5Cx10Gx4Cx42Mx2Cx5Cx3Cx17CC
Yersinia sp.	…DSDNKITA**WNWSKSF**…	Darobactins	EEQ14789.1	EEQ14794.1	Cx5Cx10Gx4Cx42Mx2Cx5Cx3Cx17CC
Pseudoalteromonas sp.	…SVAPPITA**WNWSKSF**…	Darobactins	WP_063364333.1	WP_155731785.1	Cx5Cx10Gx4Cx42Mx2Cx5Cx3Cx17CC
Vibrio spp.	…NIAPPITA**WNWSKSF**	Darobactins	WP_132940527.1	WP_156168087.1	Cx5Cx10Gx4Cx42Mx2Cx5Cx3Cx17CC
Photorhabdus asymbiotica	…TEIPEINA**WNWTKRF**…	Darobactins	WP_015834598.1	WP_015834598.1	Cx5Cx10Gx4Cx42Mx2Cx5Cx3Cx17CC
Yersinia spp.	…TLHSKITA**WSWSRSF**…	Darobactins	WP_002211950.1	WP_002227980.1	Cx5Cx10Gx4Cx42Mx2Cx5Cx3Cx17CC
Yersinia spp.	…TLRSKITA**WNWSRSF**…	Darobactins	WP_025383433.1	WP_072081216.1	Cx5Cx10Gx4Cx42Mx2Cx5Cx3Cx17CC
Yersinia bercovieri	…NFNNEITA**WSWSKSF**…	Darobactins	WP_005273871.1	WP_032897738.1	Cx5Cx10Gx4Cx42Mx2Cx5Cx3Cx17CC
Photorhabdus thracensis	…TDIPDMTT**WKWSKNL**…	Darobactins	WP_046976332.1	WP_158019997.1	Cx5Cx10Gx4Cx42Mx2Cx5Cx3Cx17CC
Photorhabdus namnaonensis	…AEIPEITA**WNWIKKF**…	Darobactins	WP_065391756.1	WP_165603325.1	Cx5Cx10Gx4Cx42Mx2Cx5Cx3Cx17CC
Martelella albus	…QENPQALG**WNWSKAF**…	Darobactins	WP_136991068.1	WP_136991070.1	Cx5Cx10Gx4Cx42Mx2Cx5Cx3Cx17CC
Sodalis praecaptivus	…AGQRQYLA**WNWSFRF**	Darobactins	WP_025420791.1	WP_025420787.1	Cx5Cx10Gx4Cx42Mx2Cx5Cx3Cx17CC
Photorhabdus laumondii	…AEIPEITA**WNWTKKF**…	Darobactins	WP_113024446.1	WP_181573423.1	Cx5Cx10Gx4Cx42Mx2Cx5Cx3Cx17CC
Candidatus Symbiopectobacterium sp.	…TISPLALA**WNWSKGF**…	Darobactins	WP_222159810.1	WP_222159813.1	Cx5Cx10Gx4Cx42Mx2Cx5Cx3Cx17CC
Serratia marcescens	…TISPTALA**WNWSKGF**…	Darobactins	Missing	WP_195314662.1	Missing N-terminus
Pseudomonadales bacterium	…KSRIPITA**WGWNRSA**…	Darobactins	MBO6565977.1	MBO6565976.1	Cx5Cx10Gx4Cx42Mx2Cx5Cx3Cx17CC
Photorhabdus luminescens	…EYENYPELSQ**WTFRF**	Daro-like (DarW)	WP_011147780.1	WP_157852141.1	Cx5Cx10Ax4Cx42Mx2Cx5Cx3Cx19CC
Photorhabdus stackebrandtii	…EYENYPELSQ**WTYRF**	Daro-like (DarW)	WP_166288413.1	WP_166288410.1	Cx5Cx10Ax4Cx42Mx2Cx5Cx3Cx19CC
Microbulbifer sp.	…PEAKSPTA**WGWGWPL**	Daro-like (DarW)	WP_108732040.1	WP_157953891.1	Cx5Cx10Gx4Cx42Mx2Cx5Cx3Cx17CC
Myxococcus sp.	…SGDEAQSA**WTWTWPF**	Daro-like (DarW)	WP_141332781.1	WP_141332782.1	Cx5Cx10Gx4Cx42Mx2Cx5Cx3Cx17CC
Sulfidibacter corallicola	…DRNDNHGK**WRWSWPF**	Daro-like (DarW)	QTD49608.1	QTD49609.1	Cx5Cx10Gx4Cx42Mx2Cx5Cx3Cx17CC
Shewanella xiamenensis	…LPKHEITN**WTWGHQF**…	Daro-like (DarW)	WP_218738443.1	WP_218738442.1	Cx5Cx10Gx4Cx42Mx2Cx5Cx3Cx19CC

Devosia sp. Leaf64	…DNQSA**WTFDIWKHSF**	Dyno-like (DynW)	WP_062629801.1	WP_062629802.1	Cx5Cx10Gx4Cx42Sx2Cx5Cx3Cx16CC
Rhizobium sullae	…TAPTM**WIFNIWKYQI**	Dyno-like (DynW)	WP_179213725.1	WP_086993390.1	Cx5Cx10Gx4Cx42Sx2Cx5Cx3Cx16CC
Rhizobium sullae	…TAPTM**WSFNIWNYRF**	Dyno-like (DynW)	WP_027510658.1	WP_027510659.1	Cx5Cx10Gx4Cx42Sx2Cx5Cx3Cx16CC
Sphingorhabdus sp.	…SAKAD**WIYNIWTYRF**	Dyno-like (DynW)	WP_164089129.1	WP_100094102.1	Cx5Cx10Gx4Cx42Fx2Cx5Cx3Cx15CC
Leptolyngbya sp.	…LLSSPG**WVFSWTYRF**	Dyno-like (DynW)	WP_172642645.1	WP_006518918.1	Cx5Cx10Gx4Cx42Mx2Cx5Cx3Cx15CC
Alphaproteobacteria bacterium	…STNDVG**WDFQWTYRF**	Dyno-like (DynW)	WP_135213304.1	WP_135213303.1	Cx5Cx10Gx4Cx42Mx2Cx5Cx3Yx17CC
Salmonella enterica	…TGG**WVNFFAKFTKSF**	XyeAB	SQI64270.1	SQI64269.1	Cx189Gx4DDALRx40Cx2Cx5Cx3Rx17C
Kosakonia cowanii	…SGG**WVNAFARWGKSF**	XyeAB	TNL01434.1	TNL01433.1	Cx189Gx4DDTLRx40Cx2Cx5Cx3Rx17C
Erwinia toletana	…SGG**WINAFANWTKRI**	XyeAB	WP_017801004.1	WP_017801003.1	Cx189Gx4DDTLRx40Cx2Cx5Cx3Rx17C
Erwinia amylovora	…SGG**WVNAFANRTMGF**…	XyeAB	WP_168428712.1	WP_168428711.1	Cx189Gx4DDTLRx40Cx2Cx5Cx3Rx17C
Erwinia aphidicola	…SGG**WVNAFARWGKSF**	XyeAB	WP_133622746.1	WP_133622747.1	Cx189Gx4DDTLRx40Cx2Cx5Cx3Rx17C
Erwinia amylovora	…SGG**WVNAFANWTKRI**	XyeAB	CCP02666.1	CCP02667.1	Cx189Gx4DDTLRx40Cx2Cx5Cx3Rx17C
Pantoea sp.	…SGG**WVNAFARWGKSF**	XyeAB	WP_187496968.1	WP_187496967.1	Cx189Gx4DDTLRx40Cx2Cx5Cx3Rx17C
Xenorhabdus sp.	…SGG**WVNAFGNWSKSL**	XyeAB	WP_099124901.1	WP_099111011.1	Cx189Gx4DDTLRx40Cx2Cx5Cx3Rx17C
Xenorhabdus spp.	…SGG**WVNAFANWSKAL**	XyeAB	WP_047680279.1	WP_072032494.1	Cx189Gx4DDTLRx40Cx2Cx5Cx3Rx17C
Photorhabdus heterorhabditis	…SGG**WVNAFAKWTKRI**	XyeAB	WP_054476436.1	WP_072161803.1	Cx190Gx4DDTLRx40Cx2Cx5Cx3Rx17C
Photorhabdus australis	…SGG**WVNAYARWTNRF**	XyeAB	WP_036768348.1	WP_072023203.1	Cx190Gx4DDTLRx40Cx2Cx5Cx3Rx17C
Xenorhabdus japonica	…SGG**WINVFARWNRAI**	XyeAB	WP_175486043.1	WP_092519408.1	Cx189Gx4DDTLRx40Cx2Cx5Cx3Rx17C
Xenorhabdus bovienii	…SGG**WVNVFARWDKAI**	XyeAB	WP_046338175.1	WP_071839243.1	Cx189Gx4DDTLRx40Cx2Cx5Cx3Rx17C
Xenorhabdus bovienii	…SGG**WLNVFVRWDRAI**	XyeAB	WP_196243385.1	WP_071826505.1	Cx189Gx4DDTLRx40Cx2Cx5Cx3Rx17C
Xenorhabdus nematophila	…SGG**WINAFGNWERAF**…	XyeAB	WP_010848442.1	WP_010848441.1	Cx189Gx4DDTLRx40Cx2Cx5Cx3Rx17C
Martelella alba	…SGG**WDNAFSRWDKKF**	XyeAB	Frameshift	WP_136988932.1	Internal Frameshift
Vibrio spp.	…SGG**WVNAFARFTKRF**	XyeAB	WP_103022078.1	WP_103022079.1	Cx189Gx4DDTLRx40Cx2Cx5Cx3Rx17C
Yersinia mollaretii	…GAG**WINAFANWTKSF**	XyeAB	WP_145520569.1	WP_073991716.1	Cx190Gx4DDTLRx40Cx2Cx5Cx3Rx17C
Yersinia mollaretii	…GAG**WINAFANWTRSF**	XyeAB	WP_049645898.1	WP_072079580.1	Cx190Gx4DDTLRx40Cx2Cx5Cx3Rx17C
Yersinia spp.	…GAG**WINAFGNWTKSF**	XyeAB	WP_050143454.1	WP_072080131.1	Cx190Gx4DDTLRx40Cx2Cx5Cx3Rx17C
Yersinia aldovae	…AGG**WVNAFLNWSKSF**	XyeAB	Missing	WP_071841501.1	Missing
Yersinia kristensenii	…AGG**WVNAFVNWPKSF**	XyeAB	WP_050115763.1	WP 072082693.1	Cx190Gx4DDTLRx40Cx2Cx5Cx3Rx17C
Yersinia spp.	…AGG**WINAFARWGRAF**	XyeAB	EEQ07318.1	EEQ07319.1	Cx190Gx4DDTLRx40Cx2Cx5Cx3Rx17C
Serratia marcescens	…SGG**WVNAFARWSRRW**	XyeAB	WP_072056065.1	WP_072056064.1	Cx189Gx4DDTLRx40Cx2Cx5Cx3Rx17C
Serratia marcescens	…SGG**WVNVFARWSRRW**	XyeAB	WP_103774053.1	WP_103774054.1	Cx189Gx4DDTLRx40Cx2Cx5Cx3Rx17C
Serratia spp.	…SGG**WVNAFARWSKSF**	XyeAB	WP_063918172.1	WP_071891933.1	Cx189Gx4DDTLRx40Cx2Cx5Cx3Rx17C
Yersinia mollaretii	…GAG**WINAFANWTKSF**	XyeAB	EEQ11988.1	EEQ11989.1	Cx190Gx4DDTLRx40Cx2Cx5Cx3Rx17C
Serratia sp.	…GAG**WIRAFANWSRSF**	XyeAB	WP_037383507.1	WP_023489715.1	Cx190Gx4DDTLRx40Cx2Cx5Cx3Rx17C
Yersinia spp.	…GAG**WIKAFGNWSRSF**	XyeAB	WP_186368484.1	WP_072088965.1	Cx190Gx4DDTLRx40Cx2Cx5Cx3Rx17C
Yersinia spp.	…AGG**WVNAFLNWSRSF**	XyeAB	WP_145584238.1	WP_145584236.1	Cx190Gx4DDTLRx40Cx2Cx5Cx3Rx17C
Yersinia frederiksenii	…AGG**WVNAFLN**	XyeAB	WP_050097262.1	WP_072086462.1	Cx190Gx4DDTLRx40Cx2Cx5Cx3Rx17C
Yersinia aleksiciae	…SGG**WVNAFLR**	XyeAB	Missing	WP_145567024.1	Missing
Yersinia frederiksenii	…AGG**WVNAFLNWPRSF**	XyeAB	WP_050317896.1	WP_072089902.1	Cx190Gx4DDTLRx40Cx2Cx5Cx3Rx17C
Yersinia spp.	…AGG**WVNAFLNWSRSF**	XyeAB	WP_128450850.1	WP_074006888.1	Cx190Gx4DDTLRx40Cx2Cx5Cx3Rx17C
Yersinia spp.	…SGG**WVNAFLRWGKSF**	XyeAB	WP_145595300.1	WP_071840519.1	Cx190Gx4DDTLRx40Cx2Cx5Cx3Rx17C
Yersinia enterocolitica	…GAG**WIKVFGNWSRSF**	XyeAB	WP_042661398.1	WP_071881823.1	Cx189Gx4DDTLRx40Cx2Cx5Cx3Rx17C
Providencia rettgeri	…SGG**WVNVFARWDKQI**	XyeAB	HBC7428735.1	HBC7428734.1	Cx189Gx4DDTLRx40Cx2Cx5Cx3Rx17C

Aeromonas jandaei	…SGG**WVNAFANWTKRF**	XyeAB	WP_201910362.1	WP_201910365.1	Cx189Gx4DDTLRx40Cx2Cx5Cx3Rx17C
Sodalis sp.	…SGG**WVNAFARWDKKF**	XyeAB	WP_213989266.1	WP_213989265.1	Cx189Gx4DDTLRx40Cx2Cx5Cx3Rx17C
Xenorhabdus sp.	…SGG**WVNAFANWSKSF**	XyeAB	WP_193850057.1	WP_193850059.1	Cx189Gx4DDTLRx40Cx2Cx5Cx3Rx17C
Mixta theicola	…GGG**WFRAYLRWSRSF**	Xye-like	WP_103059455.1	WP_165786503.1	Cx180Gx4DDILRx40Cx2Cx5Cx4Cx16C
Gilliamella sp.	…NGG**WWRAYARWRRSF**	Xye-like	WP_160406026.1	WP_160406027.1	Gx4DDILRx40Cx2Cx5Cx3Wx17C
Xenorhabdus griffiniae	…STAET**WFKLDWKKSF**	Xye-like	WP_189757994.1	WP_189757993.1	Cx191Gx4DDTLRx40Cx2Cx5Cx3Kx17C
Bordetella sp.	…ARRD**WFVKANWPRAF**	Xye-like	WP_160349802.1	WP_160349801.1	Gx4DDTLRx40Cx2Cx5Cx3Tx20C
Burkholderiales bacterium	…TKQP**WWVEASWHMAF**	Xye-like	MBV8660486.1	MBV8660485.1	Gx5DDLRNx39Cx2Cx5Cx3Kx21C
Burkholderia sp.	…NSRG**WFANATWSKAW**…	Xye-like	WP_121856868.1	WP_162999177.1	Gx5DDFRNx39Cx2Cx5Cx3Ax22C
Burkholderia sp.	…KARA**WFANASFSKRF**	Xye-like	WP_175425514.1	WP_175425513.1	Gx5DDFRNx39Cx2Cx5Cx3Tx22C
Trinickia sp.	…KPRA**WFANSSFSKRF**	Xye-like	WP_207004679.1	WP_207004678.1	Gx5DDFRNx39Cx2Cx5Cx3Ix22C
Bradyrhizobium sp.	…VSPQ**FDAWVSWTKSF**	Xye-like	WP_021082470.1	WP_021082469.1	Cx185Gx4DDFLRx40Cx2Cx5Cx3Qx17C
Pseudomonas sp.	…TTQD**FDAWISWTKSF**	Xye-like	WP_158286269.1	WP_158286270.1	Cx187Gx4DDFLRx40Cx2Cx5Cx3Qx21C
Oxalobacteraceae bacterium	…GLGA**FNAWGAWHKAI**	Xye-like	RxZ38005.1	WP_166727129.1	Cx189Gx5DDLRNx39Cx2Cx5Cx3Dx21C
Duganella sacchari	…SGEP**FNAWLAWNRTF**	Xye-like	WP_084560420.1	WP_072790966.1	Cx197Gx5DDLRNx39Cx2Cx5Cx3Dx21C
Thaumarchaeota archaeon	…SKVD**FTAWAAWTLRF**	Xye-like	MBI5145821.1	MBI5145820.1	Cx186Gx4DDLLRx40Cx2Cx5Cx3Lx17C
Pandoraea norimbergensis	…GRGNA**FVNATWSRAM**	Xye-like	WP_058376889.1	WP_157125652.1	Gx4DDTLRx40Cx2Cx5Cx3Tx20C
Pandoraea terrigena	…RSGNV**FVNATWSRAI**	Xye-like	WP_150611098.1	WP_174978392.1	Gx4DDTLRx40Cx2Cx5Cx3Tx20C
Bordetella bronchialis	…GGVGG**FANATWSKSF**	Xye-like	WP_082993604.1	WP_156770205.1	Gx4DDTLRx40Cx2Cx5Cx3Tx20C
Bordetella sp.	…GGVGG**FANASWPKSF**	Xye-like	WP_176463923.1	WP_176463924.1	Gx4DDTLRx40Cx2Cx5Cx3Tx20C
Bordetella sp.	…GGVGG**FANATWPKSF**	Xye-like	WP_086057504.1	WP_157664463.1	Gx4DDTLRx40Cx2Cx5Cx3Tx20C
Sphingobacteria sp.	…KADG**WEAWVAWNKSF**	Xye-like	MBN8828684.1	MBN8828685.1	Cx195Gx4DDTLRx38Cx2Cx5Cx3Mx17C
Methylocella tundrae	…PGRQLCG**WERWDRQK**	Xye-like	WP_174511863.1	WP_174511862.1	Cx189Gx4DDILRx39Cx2Cx5Cx3Sx17C
Photorhabdus laumondii	…VCGGGDR**WLKWIKNH**	Xye-like	WP_113025769	WP_181573497.1	Cx189Gx4DDILRx40Cx2Cx5Cx3Nx17C
Candidatus Rhabdochlamydia sp.	…THGDS**WSKNVWDRSF**	Xye-like	WP_194845874.1	WP_194845873.1	Cx189Gx4DDTLRx40Cx2Cx5Cx3Ax17C
Photorhabdus heterorhabditis	…KPGEG**WVNFTWNKSF**	Xye-like	WP_172911275.1	WP_172911276.1	Cx191Gx4DDSLRx40Cx2Cx5Cx3Rx17C
Kosakonia cowanii	…GRGEG**WVRAYWAKRF**	Xye-like	TNL02780.1	TNL02781.1	Cx189Gx4DDTLRx40Cx2Cx5Cx3Sx17C

Supplementary Table 1. Identified putative RTEs and Propeptides.
Classifies identified RiPPs into clades based upon SPASM motif. Includes NCBI accessions, an example source organism, and partial propeptide sequence. Predicted RiPP core sequence is bolded.

	C18 ACN	Phe ACN	PFP ACN	C18 MeOH	Phe MeOH	PFP MeOH
Active Well	B12 - C01	B12-C02	D09 - D12	C09 - C10	C11 - D01	E01 - E03
RT (mins)	11.5 - 12.8	11.5 - 13.3	22.3 - 24.3	16 - 17.3	17 - 18.3	24 - 26.3
Compound Mass [M], (Da)	187.0651	187.0652				
		196.124			196.1244	
	204.0919					
						210.1413
		224.1184				
	241.1450	241.1461		241.1472		
		244.182		244.1832		
		258.1029				
		260.1189		260.1209	260.1204	
	275.1295	275.1306		275.1320	275.1313	
						278.1685
			311.1552			
	313.1666	313.1666			313.1700	
					325.2051	
					327.2207	
		336.6754				
						359.1913
		384.242			384.2429	
	400.1992	400.1992		400.2029		
						410.2602
						426.2553
			438.2916			
	439.2468	439.2468		439.2507	439.2498	
			458.2604			
						474.2234
						488.2364
	496.2685	496.2235		496.2728		
						509.3300
		522.2118	552.3356	522.2165		
	523.3046	523.3046			523.3081	
						513.2891
				540.2991		
	542.2746	542.2746		542.2791	542.2786	
						545.2938
						552.3367
		557.1676				
		559.2917			559.2936	559.2741
						561.2931
	570.2697	570.2697		570.2749	570.2790	
	570.3059	570.3059			570.3101	
						574.2851
	577.2829	577.2829		577.2878		
			587.3044			
	583.3002	583.3002		583.3059		
		593.3245				
						603.3008
						618.3313
		626.371				
		641.3098				641.3495
	646.3224	646.3224			646.3267	
	655.3227	655.3227		655.3278		
			658.343			
	659.3171	659.3171		659.3229		

	661.3230	661.323		661.3284		
		664.3116				
						697.4128
	712.4178	712.4178			712.4228	
		742.4687				
	762.3856	762.3856				
	763.3632	763.3632		763.3706	763.3689	
	784.3658	784.3658				
						811.4574
						812.4416
			837.4506			
	1304.5775	1304.5775	1304.5877	1304.5890	1304.5878	1304.5901
	1489.6654	1488.6691		1488.6797	1488.6737	

Supplementary Table 2. Rapid compound identification mass table.
List of observed masses present in active wells from fractionated supernatant are listed for each separation condition. Masses conserved across all conditions are indicated in yellow highlight.

	Compound	
	1304.57	**1488.65**
Escherichia coli MG1655	16	8
Escherichia coli AR350	8	16
Salmonella enterica Enteritidis AR496	8	32
Pseudomonas aeruginosa PA01	8	16
Acinetobacter baumannii ATCC 19606	16	8
Staphylococcus aureus HG003	>128	>128
Bacillus subtilis 168	>128	>128
FaDu (pharynx, epithelial)	>1000	>1000
Hep G2 (liver, epithelial)	>1000	>1000
HEK-293 (kidney, epithelial)	>1000	>1000
A549 (lung, epithelial)	>1000	>1000
	MIC (µg/mL)	

Supplementary Table 3. MICs for dominant antimicrobial metabolites from *P. australis*

	Dynobactin A (PDB 7T3H)
Data Collection	
TEM (Voltage keV)	Thermo Fisher Arctica (200)
Wavelength (Å)	0.025079
Number of crystals	19
Data Processing	
Space group	C2
Unit cell length (Å)	42.23, 9.73, 19.07
Unit cell angles (°)	90.00, 112.00, 90.00
Resolution (Å)	10.36-1.05 (1.09-1.05)[a]
Measured reflections	59418 (9046)
Unique reflections	6485 (1300)
Redundancy	9.16 (6.96)
R_{obs}	0.205 (0.587)
R_{meas}	0.211 (0.603)
I/s	8.60 (3.51)
$CC_{1/2}$	0.990 (0.948)
Completeness (%)	98.0 (98.6)
Structure refinement	
Stoichiometric formula	$C_{60}H_{76}N_{18}O_{16}\cdot 8H_2O$
R_1	0.1294 (0.2370)
wR_2	0.3296
GooF	1.2374

[a] Values at parentheses are for the outer shell

Supplementary Table 4. Cryo-EM microED data collection and refinement statistics for dynobactin A.

Amino acid residue	Position	δ_C	δ_H
Trp	1	169.3	-
	2	55.4	3.93, m
	3	27.1	3.24, m
	4	107.2	-
	5	126.1	7.34, m
	6	136.3	-
	7		7.28, m
	8	128.4	-
	9	117.8	6.88, m
	10	117.7	7.14, m
	11	126.9	-
Asn	12	168.9	-
	13	50.4 (ovl)	4.50, br s
	14	37.9	2.60, br d (11.1) 2.67, br d (11.9)
	15	174.1	-
Ser	16	171.2	-
	17	54.7	4.03, br s
	18	58.1	3.63, m/3.59, ovl
Asn	19	171.6	-
	20	57.2	4.77, m
	21	50.4 (ovl)	4.60, m
	22	175.7	-
Val	23	173.1	-
	24	59.2	4.16, m
	25	30.6	2.01 (br s)
	26	17.5	0.89 (d, 6.7)
	27	18.4	0.87 (d, 5.4)
His	28	172.2[a]	-
	29	56.0	4.30 4.31
	30	37.0	2.56 (br s) 2.50 (br s)
	31	136.9	-
	32	135.3	8.07, m
	33	122.7	7.09, m
Ser	34	171.0[a]	-
	35	54.0	4.37, ovl
	36	59.8	3.58, m 3.44, m
Tyr	37	167.9[a]	-
	38	55.3	5.50, br d (10.4)
	39	63.4	5.52, br s
	40	123.6	-
	41	130.3	7.49, m
	42	116.7	6.89, m
	43	157.3	-
	44	116.7	6.89, m
	45	130.3	7.49, m
Arg	46	170.4	-
	47	55.8	5.03, m
	48	28.4	1.42, m

	49	23.9	1.29, m
	50	40.4	2.87, m
	51	156.5	-
Phe	52	176.3	-
	53	51.8	4.31, m
	54	37.1	2.78, m
	55	136.9	-
	56	129.4 (ovl)	6.76, br s
	57	128.4 (ovl)	7.05, m
	58	126.2	7.01, m
	59	128.4 (ovl)	7.00, m
	60	129.4 (ovl)	6.70, br s

[a]Chemical shifts can be exchangeable.

Supplementary Table 5. ^{1}H and ^{13}C NMR (900/225 MHz) chemical shift in D_2O.

	BAM-dynobactin A (EMDB-14242) (PDB 7R1W)
Data collection and processing	
Magnification	165,000x
Voltage (kV)	300
Electron exposure (e^{-}/Å^2)	48
Defocus range (μm)	0.8-3.0
Pixel size (Å)	0.82
Symmetry imposed	C1
Initial particle images (no.)	154,281
Final particle images (no.)	68,478
Map resolution (Å)	3.6
FSC threshold	0.143
Map resolution range (Å)	2.9-30
Refinement	
Initial model used (PDB code)	7NRI
Model resolution (Å)	3.9
FSC threshold	0.5
Model resolution range (Å)	2.9-9.1
Map sharpening B factor (Å^2)	79
Model composition	
Non-hydrogen atoms	11,823
Protein residues	1,499
Ligands	1
B factors (Å^2)	
Protein	114.5
Ligand	89.3
R.m.s. deviations	
Bond lengths (Å)	0.004
Bond angles (°)	0.67
Validation	
MolProbity score	1.8
Clashscore	8.2
Poor rotamers (%)	0.1
Ramachandran plot	
Favored (%)	95.5
Allowed (%)	4.5
Disallowed (%)	0

Supplementary Table 6. Cryo-EM data collection and refinement statistics of BAM-dynobactin A complex.

	BamA-β / dynobactin A
PDB Identifier	**7R1V**
Wavelength (Å)	1.000003
Resolution range (Å)	25.11–2.5 (2.59–2.5)
Space group	P 21 21 21
Unit cell	65.8 71.3 116.6
α, β, γ (°)	90 90 90
Unique reflections	19560 (1920)
Multiplicity	2.0 (2.0)
Completeness (%)	99.0 (99.5)
Mean I/sigma(I)	10.8 (1.1)
Wilson B-factor	60.9
R-merge (%)	0.026 (0.726)
Rpim (%)	0.025 (0.627)
CC1/2	1.00 (0.60)
Reflections used in Refinement	19417 (1915)
R-work	0.266 (0.389)
R-free	0.283 (0.395)
Number of atoms	3065
water	79
Protein residues	368
RMS(bonds)	0.012
RMS(angles)	1.60
Ramachandran favored (%)	95.6
Ramachandran outliers (%)	0.3
Clashscore	1.42
Average B-factor	94.5

Supplementary Table 7. X-ray diffraction data and refinement statistics of BamA-β/dynobactin A complex.

	K_d [nM] (equil.)	k_{ass} ($nM^{-1}s^{-1}$)	k_{diss} (s^{-1})	K_d [nM] (kinetic)
darobactin A	31.2 ± 1.0	0.0011	0.030	27.0 ± 1.3
darobactin B	36.2 ± 1.1	0.00050	0.014	27.1 ± 1.5
dynobactin A	2.1 ± 0.2	-[a]	0.00044	-[a]

[a] not defined, because association followed a bimodal kinetic

Supplementary Table 8. SPR measurements of BamA and ligands.